Movement of Single Myosin Filaments and Myosin Step Size on an Actin Filament Suspended in Solution by a Laser Trap

Kiwamu Saito,* Takaaki Aoki,‡ Toshiaki Aoki,‡ and Toshio Yanagida*‡

*Bio-Motron Project, Exploratory Research for Advanced Technology, Research and Development Corporation of Japan, Senba-Higashi 2-4-14, Mino, Osaka 562 and ‡Department of Biophysical Engineering, Osaka University, Toyonaka, Osaka 560, Japan

ABSTRACT   Movement of single myosin filaments, synthesized by copolymerization of intact myosin and fluorescently labeled light meromyosin, were observed along a single actin filament suspended in solution by a dual laser trap in a fluorescence microscope. The sliding velocity of the myosin filaments was 11.0 ± 0.2 μm/s at 27°C. This is similar to that of actin moving toward the center from the tip (the physiological direction) of myosin filaments bound to a glass surface but several times larger than that in the opposite direction (Ishijima and Yanagida, 1991; Yanagida, 1993). This indicates that the movement of myosin filaments is dominated by the myosin heads on one side of the myosin filament, which are correctly oriented relative to the actin filament. The incorrectly oriented myosin heads on the other side do not interfere with the fast movement. The step size (displacement produced during one ATPase cycle) of correctly oriented myosin was estimated from the minimum number of myosin heads necessary to produce the maximum velocity. This was determined by measuring the velocities of various lengths of myosin filaments. The minimum length of the myosin filaments moving near the maximum velocity was 0.30–0.40 μm, which contains 20 ± 5 correctly oriented myosin heads. This number leads to a myosin step size of 71 ± 22 nm. This value probably represents the lower limit, because all of the myosin heads on the filament would not always interact with the actin filament. Thus, the myosin step size is considerably larger than the length of a power stroke expected from the physical size of a myosin head, 10–20 nm (Huxley, 1957, 1969).

INTRODUCTION

Muscle contraction is due to the relative sliding of myosin and actin filaments (Huxley and Niedergerke, 1954; Huxley and Hanson, 1954). It has been widely believed that this sliding is driven by cyclic interactions of myosin cross-bridges with actin powered by the hydrolysis of ATP (Huxley, 1957, 1969; Huxley and Simmons, 1971). In spite of extensive investigation, however, the elementary mechanism of chemomechanical energy transduction has not been completely elucidated. Several kinds of in vitro motility assays have been developed to solve this problem (Oplatka and Tirosh, 1973; Yano, 1978; Sheetz and Spudich, 1983; Higashi-Fujime, 1985; Honda et al., 1986; Nagashima, 1986; Chaen et al., 1989; Higashi-Fujime, 1991). In particular, a myosin-coated surface motility assay, by which one can observe single fluorescently labeled actin filaments under a fluorescence microscope (Yanagida et al., 1984) and the motion produced by myosin or its subfragments bound to an artificial substrate (Kron and Spudich, 1986; Toyoshima et al., 1987; Harada et al., 1987), has been widely used.

In the present work, we have developed a new in vitro motility assay, by which we can observe the sliding movement of single myosin filaments along a single actin filament without immobilizing either protein on an artificial substrate. We combined techniques for observing highly fluorescent

individual actin and myosin filaments with a method for manipulating them under a fluorescence microscope. The optical gradient field trap, based on a highly focused laser beam, is a useful method to capture and manipulate small dielectric particles in solution (Ashkin and Dziedzic, 1987; Ashkin et al., 1987; Block, 1990; Chu, 1991). Each end of a single actin filament was bound to a 1-μm diameter latex bead caught in the laser trap. The beads were then separated until the actin filament became taut and immobilized. Single synthetic thick filaments slid along the actin filament and the velocities were measured in various experimental conditions. Thus, this new in vitro assay avoids the association between the proteins and artificial substrate.

Using this assay, we estimated the duty ratio (the probability of being in the force-generating state) and the myosin step size. In the conventional cross-bridge swinging model, it has been assumed that each interaction of a cross-bridge corresponds tightly to one ATPase cycle, independent of the load (Huxley, 1957, 1969; Huxley and Simmons, 1971; Rayment et al., 1993). Therefore, the myosin step size is expected to be limited by the size of the myosin head to approximately 20 nm (Huxley, 1969; Huxley and Simmons, 1971). In 1985, the sliding distance of actin produced by one ATPase cycle was reported to be more than 60 nm using single sarcomere preparations which had their Z line removed (Yanagida et al., 1985). Since then, the problem of whether the coupling between the power stroke and ATPase cycles is tightly determined in a one-to-one fashion has attracted a great deal of attention (Huxley, 1990; Burton, 1992; Yanagida et al., 1993; Mitsui and Ohshima, 1988; Vale and Oosawa, 1990). This problem has been extensively studied in vitro using the myosin-coated surface assay but the results

are not entirely consistent (Huxley, 1990; Burton, 1992). This is probably because the results are affected by the random orientation of myosin and the association of the myosin heads with the artificial substrate (Yanagida, 1993). It has been also argued that, when the actin filament moves along myosin heads on the surface, its leading edge approaches myosin heads that have had considerable time to reprime their ability to undergo power strokes, i.e., a considerable number of myosin heads may undergo only a part of the whole ATPase cycle to move the actin filament (Huxley, 1990). The present assay overcomes these problems because the myosin heads are regularly oriented on the filament without association with the substrate and repeatedly undergo the entire ATPase cycle during sliding.

MATERIALS AND METHODS

Sample preparation

All proteins were obtained from rabbit back skeletal muscle. G-actin was extracted from acetone powder and purified by the method of Spudich and Watt (1971). Tropomyosin was obtained by the method of Ebashi et al. (1971) and bound to actin by mixing 0.5 mg/ml tropomyosin with 1 mg/ml actin in a solution containing 150 mM KCl, 20 mM 4-(2-hydroxyethyl)-1-piperazineethanesulfonic acid (HEPES), pH 7.8. Actin or actin-tropomyosin filaments (2.5 μM in actin monomers) were labeled with phalloidin-tetramethyl-rhodamine (PHDTMR) by overnight incubation at 4°C in a solution containing 5 μM PHDTMR, 100 mM KCl, 20 mM HEPES, pH 7.8 (Harada et al., 1990). Just prior to use in each experiment, the filaments were diluted to 8.3 nM final actin monomer concentration.

Myosin was extracted from muscle by Guba-Straub solution (Guba and Straub, 1943) and purified as described by Harada et al. (1987). For storage, myosin was rapidly frozen using liquid nitrogen and kept at −80°C. N-Ethylmaleimide (NEM)-treated myosin was prepared by incubating myosin for 30 min at room temperature (25°C) in 20 mM NEM, 0.6 M KCl, and 20 mM HEPES, pH 7.0. The reaction was stopped with 0.2% 2-mercaptoethanol, and then the NEM was removed by repeated polymerization-depolymerization cycles. Light meromyosin (LMM) was obtained from myosin by the method of Szent-Györgyi et al. (1960). LMM was labeled with tetramethyl-rhodamine isothiocyanate (TRITC) by incubating 39 μM LMM with 116 μM TRITC for 3 h at 0°C in 0.6 M KCl, 50 mM HEPES, pH 7.8. Excess dye molecules were removed by gel filtration on a Sephadex G-25 column. The protein concentration of fluorescently labeled LMM was measured by the Lowry method (Lowry et al., 1951), and the concentration of bound TRITC was obtained by measuring the absorbance at 554 nm using an absorption coefficient of 84,000 M^{-1} cm^{-1}. The molar ratio of LMM to dye molecules was approximately 1:1.

Copolymers of myosin and rhodamine-labeled LMM were obtained using the method of Nagashima (1986). Myosin (0.30 mg/ml) and rhodamine-labeled LMM (83 μg/ml) were mixed at a 1:1 molar ratio (0.63 μM) in a solution containing 0.6 M KCl, 20 mM HEPES, pH 7.0, and were copolymerized by diluting them 9-fold with a low salt solution. The final solution during polymerization contained 127 mM KCl, 3 mM $MgCl_2$, 0.5 mM dithiothreitol, and 20 mM HEPES, pH 7.0. The average length of the copolymers was adjusted by changing the speed of the dilution using a variable speed micropump (Nagashima, 1986). Just prior to use in experiments, the filaments were diluted to the final concentration of 8.5 μg/ml.

The lengths of myosin filaments prepared were measured by electron microscopy. The filaments were negatively stained with uranium acetate and the negatively stained images were taken on a JEM-1200EX electron microscope (JEOL, Tokyo, Japan). The lengths of the filaments moving along the actin filament in solution were determined by measuring their fluorescence intensity using a computer image processor according to Harada et al. (1990). Comparing the fluorescence intensity of an actin filament labeled

with phalloidin tetramethyl-rhodamine at the molar ratio of 1:1, the number of LMM molecules involved in the filament was determined as q × (the fluorescence intensity of myosin filament)/(the fluorescence intensity of actin filament 1 μm long/365 subunits), where q is the ratio of the fluorescence intensity per molecule of tetramethyl-rhodamine bound to actin to that bound to LMM, which equalled 1.2. The number of myosin molecules involved is the same as that of LMM, since the copolymers contain them at the same molar ratio. The length of filament was estimated as (the total number of myosin and LMM molecules)/(3 molecules/14.3 nm), assuming that the copolymers have 3 stranded helical structure with 14.3 nm × 3 pitch (Huxley and Brown, 1967; Josephs and Harrington, 1966). The length determined agreed well with that determined by electron microscopy.

Fluorescent polystyrene latex beads, 1 μm in diameter (Ex = 530 nm, Em = 590 nm; Polysciences. Inc., Warrington, PA), were coated with NEM-treated myosin by the method of Shimmen and Yano (1984). Prior to use in experiments the myosin-coated beads were diluted to about 10^7 beads/ml in a solution containing 50 mM KCl, 4 mM $MgCl_2$, 30 μM $CaCl_2$, and 10 mM HEPES, pH 7.0.

Microscopy

Fluorescently labeled actin filaments and myosin-LMM copolymers were observed with an Olympus BH2-RFC microscope equipped with epifluorescence optics (Olympus, Tokyo, Japan), a Zeiss Neofluor 100× objective (oil immersion, NA 1.3; Carl Zeiss, Tokyo, Japan), a 100-W mercury arc lamp, and an Olympus rhodamine dichroic mirror and filter block. The fluorescence images were detected by a Hamamatsu C-2400 silicon-intensified target television camera (Hamamatsu Photonics, Hamamatsu, Japan) and stored in S-VHS format by a Victor CR6650L video cassette recorder (Victor, Tokyo, Japan) (Yanagida et al., 1984). The sliding velocity of myosin-LMM copolymers was quantified from the tape recordings using a computer image processor (Avio Excel; Nippon Avionics Co., Tokyo, Japan, and PC-9801DA; NEC, Tokyo, Japan) and special purpose software.

Dual laser optical trap apparatus

Fig. 1 shows a schematic diagram of the apparatus for manipulating single actin filaments. The infrared laser was a continuous-wave Nd:YAG laser (model 708T, wave length = 1.064 μm, mode = TEM_{00}, beam diameter $(1/e^2)$ = 1.2 mm, power = 10 mW to 8 W; Lee Laser, Inc., Orlando, FL). The laser beam was expanded to 3.6 mm in diameter by a beam expander (BE) and divided equally by a beam splitter (BS), and the beams were projected into the microscope so that beam waists (optical traps) were formed at the specimen. The position of one of the traps could be moved in the X and Y directions at the specimen by a galvanometer mirror assembly (Sasaki et al., 1991). This consisted of two orthogonal galvanometer mirror scanners (GS) and two lenses (L1 and L2). L1 and L2 had the same focal lengths, 120 mm, and were placed one focal distance from each mirror and two focal lengths from each other. The output from the scanner assembly was a collimated beam that emerged from a fixed point (rotational origin) on the second scanner mirror at an angle adjustable in both X and Y planes. The galvanometer mirror angles were controlled by a computer, and the software enabled easy manual manipulation using a computer mouse. The computer also superimposed cursors on the video raster indicating the positions of the two laser traps.

The adjustable beam was recombined with the fixed-angle beam, by a beam mixer (BM), and the two beams were passed through two lenses (L3 and L4), a half-silvered mirror (HM), and the microscope objective to the specimen plane. L3 and L4, having a focal length of 120 and 40 mm, respectively, were arranged to form an image on the scanner assembly's rotational origin at the back focal plane of the objective so as to form both beams into waists 160 mm from the objective. The distances between the scanner for the Y axis and the primary principal point of L3, the secondary principal of L3 and the primary principal of L4, and the secondary principal of L4 and the field stop of microscopy were 208, 240, and 62 mm, respectively. This placed the focus of the two beams on the same X-Y plane at
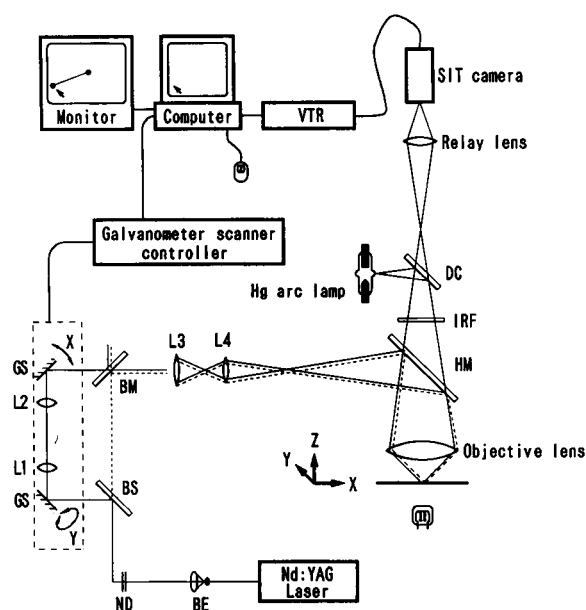
FIGURE 1 Schematic diagram of the apparatus for manipulation of individual actin filaments using dual laser traps. Nd:YAG laser, 8-W CW infrared laser; BE, beam expander; ND, neutral density filter; BS, beam splitter; GS, galvanometer scanner; L1, L2, lenses for scanning; BM, beam mixer; L3, L4, lenses for focusing; HM, half-silvered mirror; IRF, infrared filter; DC, dichroic mirror. See text for details.

the specimen when the scanners were rotated. At the specimen, the movable beam could be translated 80 μm in the X direction and 35 μm in the Y direction with a precision of 0.1 μm.

The trapping force was determined by measuring the scanning velocity at which trapped beads would be released due to the viscous drag (Ashkin et al., 1986; Block et al., 1989). The trapping force calculated as $6 \times \pi \times$ (radius of bead) $\times$ (viscosity of the solution) $\times$ (maximum scanning velocity) increased almost linearly with laser beam power. The laser beam power was measured by a thermal disc power meter (model 210; Coherent, Palo Alto, CA). Using 1-μm diameter beads, the trapping force was 130 pN at 0.37-W laser power per beam at the specimen.

Manipulation of an actin filament

When an actin filament was manipulated, 1 μl of solution containing actin filaments labeled with fluorescent phalloidin (8.3 nM in actin monomers) and 1 μl of solution containing latex beads coated with NEM-myosin (10^7 beads/ml) were mixed with 15 μl of a solution containing 25 mM KCl, 3 mM MgCl$_2$, 2 mM ATP, and 20 mM HEPES, pH 7.8, on a glass slide of which surface had been treated with silicone (Sigmacote; Sigma Chemical Co., St. Louis, MO) (Harada et al., 1987, 1990). To minimize photobleaching, an oxygen-depletion system (1% 2-mercaptoethanol, 4.5 mg of glucose/ml, 216 μg of glucose oxidase/ml, and 36 μg catalase/ml, final concentrations) was added to the solution in all experiments (Harada et al., 1990). An 18 $\times$ 18 mm^2 overslip, also coated with silicone, was placed over the droplet, and the edges were sealed with nail polish. Single latex beads were trapped in each of the two laser beams (Fig. 2 A). One end of an actin filament was attached to the bead trapped in the movable laser beam (Fig. 2 B), and then the other end of the filament was brought into contact with the fixed-position bead by manipulating the microscope stage and the movable trap. The position of the movable trap was adjusted until the suspended actin filament was horizontal in the video image and not slack. The vertical (Z-axis) position of the suspended actin filament could be manipulated along with the plane of focus by altering the microscope objective focus. Fig. 2 D schematically shows the actin filament held between the beads trapped in the laser beams.
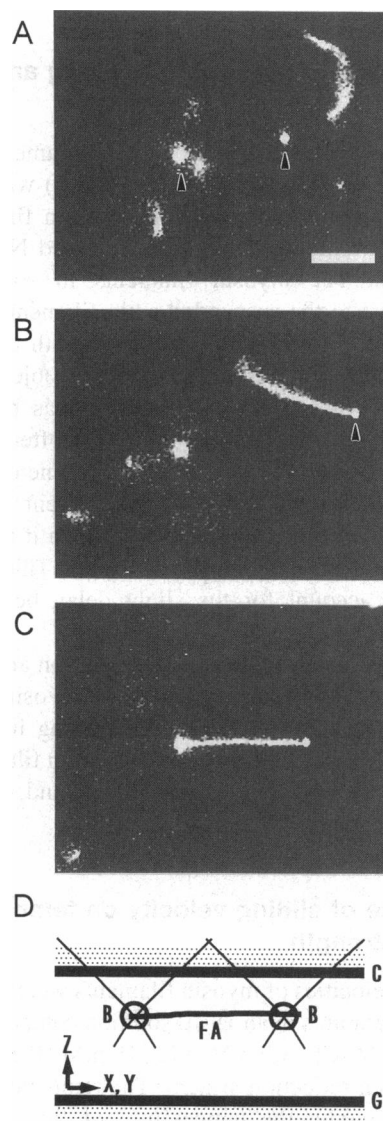

FIGURE 2 Manipulation of an actin filament. (A) Two fluorescent latex beads, indicated by arrow heads, were trapped at the focal spots of the two laser beams. An actin filament, labeled with fluorescent phalloidin, can be seen in the upper right-hand side. It took only a few minutes to get an actin filament with two beads on it. The scale bar is 10 μm. (B) One bead (marked by a single arrow head) was brought into contact and bound tightly with one end of the actin filament by moving the focal spot with the mirrors mounted on the galvanometer scanners (see Fig. 1). The bead was precoated with NEM-treated myosin to increase the affinity for actin. (C) The other free end of the actin filament was attached to another bead trapped at the fixed laser beam. The two traps were separated until the actin filament became taut. (D) Schematic diagram of the actin filament suspended in solution by the laser traps. FA, actin filament; B, beads coated with NEM-treated myosin; CS, coverslip; GS, glass slide.

The temperature of the solution was not expected to increase appreciably because of irradiation by the laser beam. We tested this point by measuring the velocity of actin filaments near the beam using the myosin-coated surface assay (Harada et al., 1990). Long periods (5 min) of irradiation by the laser beam did not increase the velocity, although velocity is very sensitive to temperature (Q_{10} = 2.5) (Harada et al., 1990). Furthermore, direct irradiation of the actin filaments and the myosin filament by the laser beam neither affected their motility nor bleached the bound fluorescent dye.

RESULTS

Movement of myosin filaments along an actin filament

When the movement of single myosin filaments (copolymers of myosin and TRITC-labeled LMM) was to be observed, 1 μl of solution containing myosin filaments was added to the mixture of actin filaments and NEM-myosin coated beads. The myosin filaments in solution were moved relative to the suspended actin filament by moving the glass slide on the microscope stage with the positions of the laser beams fixed and by altering objective focussing control. When a myosin filament was brought into contact with the actin filament there was often a brief delay (0.1–0.5 s), and then it moved toward one of the beads. The initial attachment of a myosin filament to the actin was presumably at a random angle but then it aligned with the actin filament and began to move. This alignment process may account for the slight delay before motion commenced.

Fig. 3 shows a myosin filament in solution and then after attaching to an actin filament with tropomyosin suspended between two beads. The velocity of sliding in the steady phase was 11.0 μm/s at 25°C. For each actin filament, myosin filaments always translated toward one end, even though the myosin filaments were bipolar.

Dependence of sliding velocity on temperature and ionic strength

The sliding velocities of myosin filaments were measured at various temperatures in an 18-μl solution containing 36 mM KCl, 2.9 mM $MgCl_2$, 1.7 mM ATP, 19 mM HEPES, pH 7.8, and the oxygen-reduction system. The temperature was adjusted by changing the temperature of the experimental room. The temperature of the solutions was measured by a thermocouple with a diameter of 150 μm. The velocities increased to 5.4 ± 0.1 μm/s (mean ± SE, $n = 40$), 8.9 ± 0.2 μm/s ($n = 39$), 10.5 ± 0.2 μm/s ($n = 102$), and 13.9 ± 0.3 μm/s ($n = 40$) at 20, 25, 27, and 30°C, respectively (Fig. 4, open circles). The Q_{10} was 2.6. When tropomyosin was bound to F-actin, the sliding velocities increased to 6.7 ± 0.1 ($n = 39$), 11.3 ± 0.2 ($n = 43$), and 15.4 ± 0.3 ($n = 30$) μm/s at 20, 25, and 30°C, respectively (Fig. 4, filled circles).

Fig. 5 shows the velocities at various concentrations of KCl. The sliding velocity increased from 6.2 to 10.6 μm/s when the concentration of KCl was varied from 15 to 78 mM at 25°C. At 98 mM KCl, even when myosin filaments were pushed into contact with the actin filament, they did not move.

Dependence of sliding velocity on length of myosin filaments

Short copolymer filaments of myosin and fluorescently labeled LMM were made by rapid dilution (see Materials and Methods). Fig. 6 shows the length distribution of filaments
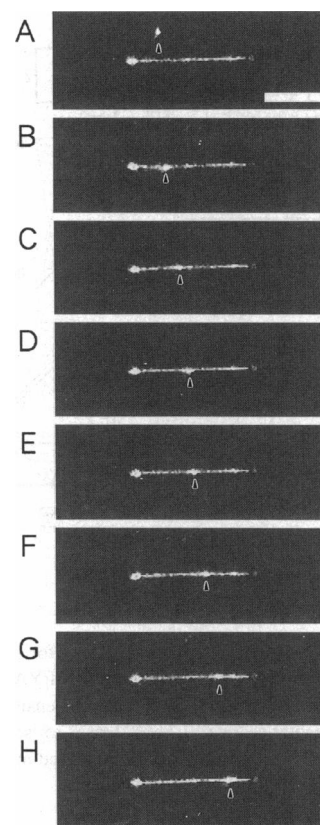

FIGURE 3 Sequential fluorescence micrographs of a myosin filament (a copolymer with fluorescently labeled LMM) sliding along an actin-tropomyosin complex suspended in solution by the laser traps. (*A*) A myosin filament floating in solution (marked by an *arrowhead*) is being moved toward the actin filament by moving the microscope stage. It attaches to the actin filament (*B*) and begins to move (sometimes after a brief pause) (C—H) (*arrowheads*). The velocity was determined by measuring sliding distance (> 3 μm) of filaments and time. Medium: 36 mM KCl, 29 mM $MgCl_2$, 1.7 mM ATP, 19 mM HEPES, pH 7.8. The temperature was 25 ± 1°C. The scale bar is 10 μm. The images in *B* to *H* were taken 200 ms apart.

determined by electron microscopy. The lengths distributed from 0.30 to 1.1 μm, and the average length was 0.56 μm. This distribution is similar to that of pure myosin filaments made by rapid dilution (Huxley and Brown, 1967). Fig. 7 *a* shows the velocities of the various lengths of copolymers. The lengths of copolymers moving along the actin filament were determined by measuring the fluorescence intensity as described in Materials and Methods. In this case the fluorescence of the actin had to be subtracted (see Fig. 3), so the actin filaments were labeled with nonfluorescent phalloidin and fluorescent phalloidin at the molar ratio of 5:1. The velocity was constant until the length decreased to 0.5 μm. The shorter filaments easily detached from the actin filament and did not move continuously. This is probably due to the decrease in the total number of myosin heads, so that a myosin filament could not interact continuously with the actin filament due to Brownian motion. In order to suppress the Brownian motion, the viscosity of solution was increased by adding methylcellulose (Uyeda et al., 1990). The minimum lengths of the filaments moving at the maximum velocity
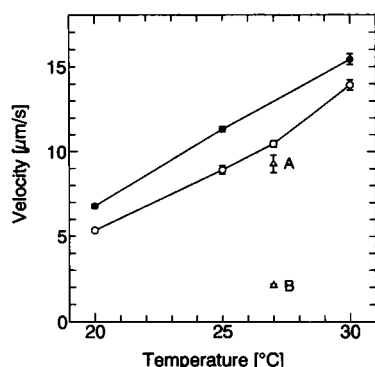
FIGURE 4   Dependence of the sliding velocity on the temperature. The velocities are plotted for myosin-LMM copolymers sliding along actin filaments (O) and the actin-tropomyosin complexes (●). The bar represents the standard error of the mean for 30–43 copolymers. Medium: 36 mM KCl, 29 mM MgCl$_2$, 1.7 mM ATP, 19 mM HEPES, pH 7.8, and the oxygen-reduction system. The length of myosin filaments used was 2–4 μm. The velocities of actin along myosin-rod copolymer filaments in the normal direction ($\triangle$, A) and the opposite direction ($\triangle$, B) obtained in the same solution (Yanagida et al., in press) are also shown.

FIGURE 6   Distribution of myosin-LMM copolymer length. The distribution was obtained from negatively stained electron microscope images. The number of filaments counted was 244.
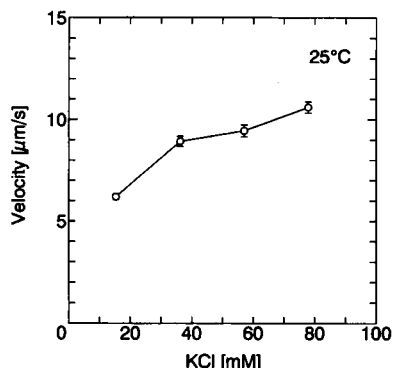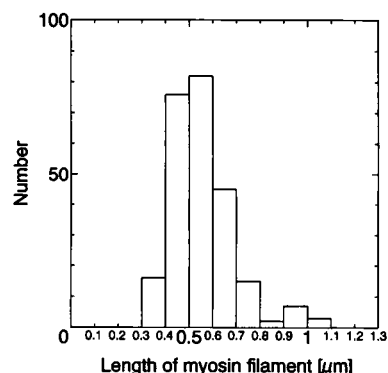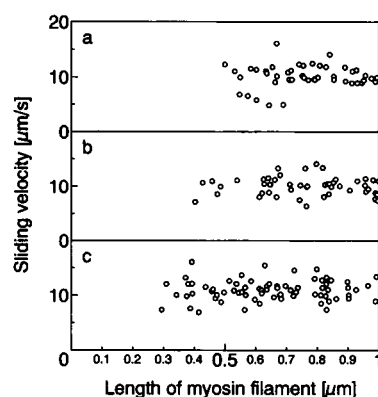

FIGURE 5   Dependence of the sliding velocity on ionic strength. The ionic strength was adjusted by changing the concentration of KCl in a solution containing 2.9 mM MgCl$_2$, 1.7 mM ATP, 19 mM HEPES, pH 7.8, and the oxygen-reduction system. The bar gives the standard error of the mean for 34–39 copolymers. The temperature was 25 ± 1°C. The length of myosin filaments was 2–4 μm.

FIGURE 7   Sliding velocities of myosin-LMM copolymer of various lengths on the actin filament. Medium: 36 mM KCl, 29 mM MgCl$_2$, 1.7 mM ATP, 19 mM HEPES, pH 7.8, the oxygen-reduction system and 0% (a), 0.1% (b), 0.3% (c) methylcellulose. The temperature was 27 ± 1°C.

decreased to 0.40 and 0.30 μm at 0.1 and 0.3% methylcellulose, respectively (Fig. 7, b and c). As the minimum length obtained, 0.30 μm, is the same as the minimum length of myosin filaments used (Fig. 6), the minimum length of filament needed to move at the maximum velocity must be shorter than 0.30 μm.

Duty ratio and myosin step size

We estimated the duty ratio and the step size of myosin heads interacting in the correct (the physiological) orientation with the actin filament from the dependence of velocity of myosin filaments on its length. The velocity of the short myosin filaments (0.30–0.40 μm) was 11.5 ± 0.8 μm/s (mean ± SE; $n = 11$) in the presence of 0.3% methylcellulose. This velocity was 0.105 ± 0.008 of that of filaments more than 0.4 μm long (11.0 ± 0.2 μm/s; mean ± SE; $n = 68$; Fig. 7 c).

The number of correctly oriented myosin heads on one side of a filament 0.30–0.40 μm long was estimated to be 20 ± 5 from the fluorescence measurements (see Materials and Methods). Since the sliding velocity (v) at zero load is independent of the number of myosin heads that exert the sliding force on the actin at the same time and is proportional to the probability that at least one head exerts the sliding force, v is given as

$$v = v_o \times \{1 - (1 - f)^N\}, \tag{1}$$

where v_o is the maximum velocity when the number of myosin heads (N) that can interact with the actin is large, and f is the duty ratio (the probability of being in the force generating state) (Harada et al., 1990; Uyeda et al., 1990). We consider 0.97, the minimum value of v/v_o (0.105 ± 0.008) for the length of myosin filaments of 0.30–0.40 μm, which gives the lower limit of f. Inserting this value and the number of heads $N = 20 ± 5$ into the Eq. 1, the duty ratio is calculated as $f = 0.16 ± 0.04$.

The myosin step size (d) is obtained as

$$d = v_o \times (f/V_{ATP}), \tag{2}$$

where V_{ATP} is the ATPase activity during sliding (Harada et al., 1990; Uyeda et al., 1990; Toyoshima et al., 1990). The ATPase activity could not be determined using the present in vitro system. We used the maximum actin-activated ATPase activities of double-headed myosin subfragment, HMM, or myosin minifilament in solution as V_{ATP}. V_{ATP} is expected not to be larger than the maximum ATPase activity of myosin at infinite actin concentration. The interaction between actin and myosin suspended in solution may be different from that during sliding between actin and myosin filaments. But, recent studies have suggested that the ATPase activity of muscle myofibrils or fibers during sliding at low or zero load is small (Harada et al., 1990; Ohno and Kodama, 1991; Higuchi and Goldman, 1991). Furthermore, Reisler (1980) has showed that the ATPase activity of acto-HMM suspension is almost the same as that when myosin forms filaments (minifilament). Thus, when the maximum ATPase activity in solution is used as V_{ATP}, the myosin step size would be calculated to be similar to or lower than the true value. Extrapolating values of the acto-HMM and acto-myosin minifilament ATPase activities previously reported (Reisler, 1980; Margossian and Lowey, 1973; Wagner and Giniger, 1981) to 27°C using $Q_{10} = 4.5$ (Margossian and Lowey, 1973) and the acto-HMM ATPase activity obtained under the same conditions (20 s^{-1} $head^{-1}$, Harada, unpublished data) range from 20 to 30 s^{-1} $head^{-1}$. Inserting V_{ATP} = 25 ± 5 s^{-1} $head^{-1}$ and f = 0.16 ± 0.04 into the Eq. 2, the myosin step size, d is calculated as

$$d = (11.0 \pm 0.2 \ \mu m \ s^{-1}) \times \left(\frac{0.16 \pm 0.04}{25 \pm 5} \ s^{-1} \ head^{-1} \right)$$

$$= 71 \pm 22 \ nm.$$

This shows the mean ± possible error. The possible error ($\{\sum [\sigma_i^2 (\partial \mu' / \partial x_i)^2]\}^{1/2}$, σ_i, the variance of the individual data point x_i; μ', the mean) was calculated by the general method described by Bevington (1969). This value is probably the lower limit as the minimum value of v/v_o was used, as mentioned. Furthermore, the steric arrangement of the myosin heads against the actin filament would considerably limit the number of myosin heads that orient toward the actin filament and can interact with it as the myosin heads project radially from the filament. Thus, the number of myosin heads that can interact with actin filament would be two to three times smaller than the total number of myosin heads on the filament. If correct, the minimum number of myosin heads would be 8–13, and the duty ratio and the myosin step size would be 0.24–0.36 and 93–169 nm, respectively.

DISCUSSION

The technique presented here extends the techniques developed recently for investigating energy transduction by motor proteins. In 1984, it was demonstrated that single actin filaments, stabilized with the highly fluorescent tetramethylrhodamine phalloidin, can be observed clearly by fluorescence microscopy. This development has enabled the motions of single actin filaments to be visualized during the

interaction with myosin or its subfragments in the presence of ATP (Yanagida et al., 1984). Spudich and colleagues obtained unidirectional movement of actin interacting with myosin and its subfragments fixed on a substrate such as a glass surface or nitrocellulose film (Kron et al., 1986; Toyoshima et al., 1987). This myosin-coated surface motility assay is simple and does not require special apparatus or skill, and it has been widely adopted. Harada et al. (1987) found that the double-headed structure of the myosin molecule is not essential to move actin and, furthermore, Toyoshima et al. (1987) demonstrated that S-1 alone is sufficient to move actin. Kishino et al. (1988) developed a technique for force measurement in this assay and showed that S-1 can produce not only motion but also force. The myosin-coated motility assay has also been used to extensively investigate activities of smooth and nonmuscle motor proteins (Sellers and Kachar, 1990; Ishikawa et al., 1991; Okagaki et al., 1991; Umemoto et al., 1989; Warshaw et al., 1991), and artificially expressed proteins (Manstein et al., 1989; Sutoh et al., 1991).

Recently, several disadvantages of the myosin-coated surface assay have been identified. The number of heads on the surface that can take part in effective generation of sliding force is uncertain because the heads are randomly arranged on the surface and they may be chemically and/or mechanically affected by interaction with the surface. Reported sliding velocities have varied substantially and are strongly dependent on the preparation and condition of the myosin or myosin subfragments-coated surface (see review, Higashi-Fujime (1991)). At 30°C, for example, the velocity of actin on monomeric myosin bound to a silicone-coated glass surface was reported to be 11 $\mu m/s$ (Harada et al., 1990), while the velocities of monomeric myosin and heavy meromyosin bound to a collodion (nitrocellulose) film were reported to be in the ranges 3.5–7.2 $\mu m/s$ (Toyoshima et al., 1987; Uyeda et al., 1990; Toyoshima et al., 1990). The force has been found to be ever more greatly dependent on the surface (Ishijima et al., in preparation). The effects of the orientation and interactions with artificial substrates need to be understood for quantitative analyses such as estimation of the myosin step size.

These problems can be overcome by measuring the sliding velocity of myosin filaments along actin filaments in solution. Previously, Fujime observed the sliding movement of myosin filaments along bundles of actin filaments formed at high $MgCl_2$ concentration (~20 mM) (Higashi-Fujime, 1985) but the movement was limited and unphysiological. Nagashima (1986) observed the motion of myosin filaments at high densities of actin filaments under a dark-field microscope, but the myosin filaments rarely moved and not continuously or smoothly.

The optical gradient trap has enabled us to immobilize individual actin filaments in solution using a pair of latex beads. Ashkin and colleagues demonstrated that focussed infrared laser light could trap living cells and organelles or filaments in a cell without apparent damage (Ashkin and Dziedzic, 1987; Ashkin et al., 1987; Ashkin and Dziedzic,

1989), and it has been used for manipulating biological materials (Block et al., 1989, 1990; Kucik et al., 1991; Svoboda et al., 1992). With submicron particles, the laser trap can produce forces in the range of several tens of piconewtons, considerably higher than the force produced by single motor proteins (Kishino and Yanagida, 1988; Ishijima et al., 1991). This characteristic feature enables the use of the optical trap for measuring the force produced by microtubule-based motor proteins attached to an organelle (Ashkin et al., 1990) or to a small bead (Block et al., 1990; Kuo and Sheetz, 1993). However, diffraction prevents this method from being applied to trap objects much smaller than the wavelength of the laser light (Ashkin et al., 1986). Therefore, actin filaments, about 8 nm in diameter (Hanson and Lowy, 1963), were captured by attaching them to small latex beads. This technique is similar to that applied to DNA (Chu, 1991; Kucik et al., 1991; Svoboda et al., 1992).

The present system has enabled reproducible observation of the smooth and continuous movement of myosin filaments along actin filaments. Since the actin and myosin were free from interaction with the surface, the sliding velocity was almost constant in each experiment under the same conditions. The velocities of 5.4 μm/s at 20°C and 14 μm/s at 30°C obtained here are close to those in skinned rabbit psoas fibers (Higuchi et al., unpublished).

Since the myosin filaments have a bipolar structure, the myosin heads on one half side are oriented in the normal direction with respect to the actin filament, but those on the other are oriented in the opposite direction. Recently, Reedy et al. (1989) and Toyoshima et al. (1989) suggested that myosin molecules are flexible enough to interact with the actin in any direction. Sellers et al. (1990) and Yamada et al. (1990) have demonstrated with giant thick filaments from molluscan smooth muscle that actin can move not only toward the center of the thick filament but also away from the center. The latter velocity, however, was about 10 times slower than the former. In all of these experiments the direction of motion was determined by the polarity of the actin filament. These points were confirmed using synthetic thick filaments of rabbit skeletal muscle (Ishijima and Yanagida, 1991; Yamada and Wakabayashi, 1993).

In our experiments, the thick filaments moved as fast as in the skinned muscle fiber, where the actin is moved only by the correctly oriented myosin heads. Furthermore, the velocity of thick filaments was almost the same as that of actin filaments toward the center (normal direction) of co-polymer filaments bound to a coverslip under the same medium conditions (Fig. 4). This indicates that when myosin heads oriented in both directions interact with actin simultaneously, the movement is dominated by the correctly oriented myosin heads and the incorrectly oriented ones do not interfere with the fast movement and do not impose friction. This result agrees with those obtained with molluscan smooth muscle myosin (Sellers et al., 1991; Yamada and Takahashi, 1992). Since the contribution of myosin heads oriented in the incorrect direction for the movement of actin

is negligible, the movement produced by correctly oriented heads can be studied in the present assay.

Using this assay, we showed that the step size of myosin heads in the correct (the physiological) orientation with the actin filament was at least 72 ± 22 nm, probably > 100 nm. Recently, we have shown by force and displacement recordings directly from single myosin heads in vitro that the displacement caused by a single interaction of a cross-bridge is approximately 17 nm at zero load (Ishijima et al., submitted data). The results indicate that the cross-bridge undergoes many force-generating interactions during one ATPase cycle at zero load. Thus, the coupling between the mechanical and ATPase cycles is not determined rigidly in a one-to-one fashion, in disagreement with the conventional 1:1 tight coupling hypothesis (Huxley, 1957, 1969). In the previous studies using the myosin or HMM-coated surface, the results on the myosin step size are not entirely consistent. We have reported using myosin-coated coverslips, which had been previously treated with silicone that the duty ratio is ~0.5, and the step size is >100 nm at zero load (Yanagida, 1993; Harada et al., 1990). Spudich and colleagues have reported, using HMM-coated nitrocellulose film, that the duty ratio is ~0.05 and the myosin step size is 5–28 nm at zero load, which are consistent with the conventional 1:1 hypothesis (Uyeda et al., 1990, 1991; Toyoshima et al., 1990). These studies have estimated the number of myosin heads that can interact with the actin from the density of myosin heads or from the actin-activated myosin or HMM ATPase activity on the surface. The analysis assumes that all myosin heads near the actin filament or showing ATPase activity can produce normal fast movement. This assumption ignores the possibility that significant numbers of myosin or HMM, which are randomly arranged on the surface, may be unable to interact in the correct orientation with the actin and may be inactivated by interaction with the surface. The force have been found to be greatly dependent on how myosin or HMM are bound to surfaces. This suggests that the number of effective myosin heads that can produce normal fast movement varies greatly depending on the surface, even though the densities of myosin heads bound to them are similar (Ishijima et al., submitted). It has been recently suggested that the discrepancy in the previous in vitro studies could be explained, if the number of the effective myosin heads is estimated not from the density of myosin heads but from the force developed on the surface; namely, the myosin step sizes thus recalculated are >100 nm (Yanagida, 1993).

Recently, the mechanical and structural studies on muscle have also showed that the sliding distance of actin during one ATPase cycle at low load is considerably larger than the length of a single power stroke expected from the physical size of a myosin head, 10–20 nm (Ohno and Kodama 1991; Higuchi and Goldman, 1991; Lombardi et al., 1992; Irving et al., 1992; Burton and Simmons, 1991; Brenner, 1991; Yamada et al., 1993). There are two types of mechanisms to explain the one to many coupling between the ATPase and power stroke cycles; one is that a myosin head produces many power strokes during one ATPase cycle; and another

is that myosin heads undergoing a power stroke utilizing ATP induce several cost-free power strokes of other heads via mechanical coupling through the filaments (Yanagida et al., 1985). Recently, Cooke et al. (submitted) has proposed the weak coupling model based on the latter mechanism to explain the large sliding distance observed in isotonically contracting muscle fibers at low load. However, the latter mechanism could not be applied to that observed in in vitro assays, because the latter mechanism would need a large number of myosin heads that at least one head undergoes a power stroke utilizing ATP at any moment. Thus, during rapid sliding at low load, chemomechanical coupling between the ATPase and power stroke cycles is not simply explained by a conventional one-to-one coupling hypothesis but an entirely new mechanism may be needed to explain it (Yanagida et al., 1993).

REFERENCES

Ashkin, A., J. M. Dziedzic, J. E. Bjorkholm, and S. Chu. 1986. Observation of a single-beam gradient force optical trap for dielectric particles. *Opt. Lett.* 11:288–290.

Ashkin, A., and J. M. Dziedzic. 1987. Optical trapping and manipulation of viruses and bacteria. *Science (Wash. DC)*. 235:1517–1520.

Ashkin, A., J. M. Dziedzic, and T. Yamane. 1987. Optical trapping and manipulation of single cells using infrared laser beams. *Nature (Lond.)*. 330:769–771.

Ashkin, A., and J. M. Dziedzic. 1989. Internal cell manipulation using infrared lasertraps. *Proc. Natl. Acad. Sci. USA*. 86:7914–7918.

Ashkin, A., K. Schütze, J. M. Dziedzic, U. Euteneuer, and M. Schliwa. 1990. Force generation of organelle transport measured in vivo by an infrared laser trap. *Nature (Lond.)*. 348:346–348.

Bevington, P. R. 1969. Data Reduction and Error Analysis for the Physical Sciences. McGraw-Hill/New York. Chap. 5.

Block, S. M. 1990. Optical tweezers: a new tool for biophysics. *In* Noninvasive Techniques in Cell Biology. J. K. Foskett and S. Grinstein, editors. Wiley-Liss/New York. pp. 375–402.

Block, S. M., D. F. Blair, and H. C. Berg. 1989. Compliance of bacterial flagella measured with optical tweezers. *Nature (Lond.)*. 338:514–517.

Block, S. M., L. S. B. Goldstein, and B. J. Schnapp. 1990. Bead movement by single kinesin molecules studied with optical tweezers. *Nature (Lond.)*. 348:348–352.

Brenner, B. 1991. Rapid dissociation and reassociation of actomyosin crossbridges during force generation: a newly observed facet of cross-bridge action in muscle. *Proc. Natl. Acad. Sci. USA*. 88:10490–10494.

Burton, K. 1992. Myosin step size: estimates from motility assays and shortening muscle. *J. Muscle Res. Cell Motil.* 13:590–607.

Burton, K., and R. M. Simmons. 1991. Changes in stiffness during the transition from the isometric state to steady shortening in skinned fibers isolated from rabbit psoas muscle. *J. Physiol. (Lond.)*. 434:63P.

Chaen, S., K. Oiwa, T. Shimmen, H. Iwamoto, and H. Sugi. 1989. Simultaneous recordings of force and sliding movement between a myosin-coated glass microneedle and actin cables in vitro. *Proc. Natl. Acad. Sci. USA*. 86:1510–1514.

Chu, S. 1991. Laser manipulation of atoms and particles. *Science (Wash. DC)*. 253:861–866.

Ebashi, S., T. Wakabayashi, and F. Ebashi. 1971. Troponin and its components. *J. Biochem.* 69:441–445.

Guba, F., and F. B. Straub. 1943. Extraction of myosin. *Studies*. 3:46–48.

Hanson, J., and J. Lowy. 1963. The structure of F-actin and of actin filaments isolated from muscle. *J. Mol. Biol.* 6:46–60.

Harada, Y., A. Noguchi, A. Kishino, and T. Yanagida. 1987. Sliding movement of single actin filaments on one-headed myosin filaments. *Nature (Lond.)*. 326:805–808.

Harada, Y., K. Sakurada, T. Aoki, D. D. Thomas, and T. Yanagida. 1990. Mechanochemical coupling in actomyosin energy transduction studied by in vitro movement assay. *J. Mol. Biol.* 216:49–68.

Higashi-Fujime, S. 1985. Unidirectional sliding of myosin filaments along the bundle of F-actin filaments spontaneously formed during superprecipitation. *J. Cell Biol.* 101:2335–2344.

Higashi-Fujime, S. 1991. Reconstitution of active movement in vitro bead on the actin-myosin interaction. *Int. Rev. Cytol.* 125:95–138.

Higuchi, H., and Y. E. Goldman. 1991. Sliding distance between actin and myosin filaments per ATP molecule hydrolysed in skinned muscle fibers. *Nature (Lond.)*. 352:352–354.

Honda, H., H. Nagashima, and S. Asakura. 1986. Directional movement of F-actin in vitro. *J. Mol. Biol.* 191:131–133.

Huxley, A. F. 1957. Muscle structure and theories of contraction. *Progr. Biophys. Biophys. Chem.* 7:255–318.

Huxley, H. E., 1969. The mechanism of muscular contraction. *Science (Wash. DC)*. 164:1356–1365.

Huxley, H. E. 1990. Sliding filaments and molecular motile systems. *J. Biol. Chem.* 265:8347–8350.

Huxley, H. E., and W. Brown. 1967. The low-angle X-ray diagram of vertebrate striated muscle and its behavior during contraction and rigor. *J. Mol. Biol.* 30:383–434.

Huxley, H. E., and J. Hanson. 1954. Changes in the cross-striations of muscle during contraction and stretch and their structural interpretation. *Nature (Lond.)*. 173:973–976.

Huxley, A. F., and R. Niedergerke. 1954. Structural changes in muscle during contraction: interference microscopy of living muscle fibres. *Nature (Lond.)*. 173:971–973.

Huxley, A. F., and R. M. Simmons. 1971. Proposed mechanism of force generation in striated muscle. *Nature (Lond.)*. 233:533–538.

Irving, M., V. Lombardi, G. Piazzesi, and M. A. Ferenczi. 1992. Myosin head movements are synchronous with the elementary force-generating process in muscle. *Nature (Lond.)*. 357:156–158.

Ishijima, A., T. Doi, K. Sakurada, and T. Yanagida. 1991. Sub-piconewton force fluctuations of actomyosin in vitro. *Nature (Lond.)*. 352:301–306.

Ishijima, A, and T. Yanagida. 1991. Force fluctuations on a single actin filament—interaction with oriented myosin molecules. *Proc. 29th Japan Biophys. Sci. Meeting.* S195 (in Japanese).

Ishikawa, R., T. Okagaki, S. Higashi-Fujime, and K. Kohama. 1991. Stimulation of the interaction between actin and myosin by *Physarum* caldesmon-like protein and smooth muscle caldesmon. *J. Biol. Chem.* 266:21784–21790.

Josephs, R., and W. F. Harrington. 1966. Studies on the formation and physical chemical properties of synthetic myosin filaments. *Biochemistry.* 5:3474–3487.

Kishino, A., and T. Yanagida. 1988. Force measurements by micromanipulation of a single actin filament by glass needles. *Nature (Lond.)*. 334:74–76.

Kron, S. J., and J. A. Spudich. 1986. Fluorescent actin filaments move on myosin fixed to a glass surface. *Proc. Natl. Acad. Sci. USA*. 83:6272–6276.

Kucik, D. F., S. C. Kuo, E. L. Elson, and M. P. Sheetz. 1991. Preferential attachment of membrane glycoproteins to the cytoskeleton at the leading edge of lamella. *J. Cell Biol.* 114:1029–1036.

Kuo, S. C., and M. P. Sheetz. 1993. Force of single kinesin molecules measured with optical tweezers. *Science (Wash. DC)*. 260:232–234.

Lombardi, V., G. Piazzesi, and M. Linari. 1992. Rapid regeneration of the actin-myosin power stroke in contracting muscle. *Nature (Lond.)*. 355:638–641.

Lowry, O. H., N. J. Rosebrough, A. L. Farr, and R. J. Randall. 1951. Protein measurement with the folin phenol reagent. *J. Biol. Chem.* 193:265–275.

Manstein, D. J., K. M. Ruppel, and J. A. Spudich. 1989. Expression and characterization of a functional myosin head fragment in *Dictyostelium discoideum*. *Science (Wash. DC)*. 246:656–658.

Margossian, S. S., and S. Lowey. 1973. Substructure of the myosin molecule. IV. Interactions of myosin and its subfragments with adenosine triphosphate and F-actin. *J. Mol. Biol.* 74:313–330.

Mitsui, T., and H. Ohshima. 1988. A self-induced translation model of myosin head motion in contracting muscle. 1. Force-velocity relation and energy liberation. *J. Muscle Res. Cell Motil.* 9:248–260.

Nagashima, H. 1986. Active movement of synthetic myosin filaments observed by dark-field light microscopy. *J. Biochem.* 100:1023–1029.

Ohno, T., and T. Kodama. 1991. Kinetics of adenosine triphosphate hydrolysis by shortening myofibrils from rabbit psoas muscle. *J. Physiol. (Lond.).* 441:685–702.

Okagaki, T., S. Higashi-Fujime, R. Ishikawa, H. Takano-Ohmuro, and K. Kohama. 1991. In vitro movement of actin filaments on gizzard smooth muscle myosin: requirement of phosphorylation of myosin light chain and effects of tropomyosin and caldesmon. *J. Biochem.* 109:858–866.

Oplatka, A., and R. Tirosh. 1973. Active streaming in actomyosin solutions. *Biochim. Biophys. Acta.* 305:684–688.

Rayment, I., H. M. Holden, M. Whittaker, C. B. Yohn, M. Lorentz, K. C. Holmes, and R. A. Milligan. 1993. Structure of the actin-myosin complex and its implications for muscle contraction. *Science (Wash. DC).* 261: 58–65.

Reedy, M. C., C. Beall, and E. Fyrberg. 1989. Formation of reverse rigor chevrons by myosin heads. *Nature (Lond.).* 339:481–483.

Reisler, E. 1980. Kinetic studies with synthetic myosin minifilaments show the equivalence of actomyosin and acto-HMM ATPases. *J. Biol. Chem.* 255:9541–9544.

Sasaki, K., M. Koshioka, H. Misawa, N. Kitamura, and H. Masuhara. 1991. Laser-scanning micromanipulation and spatial patterning of fine particles. *Jpn. J. Appl. Phys.* 30:L907-L909.

Sellers, J. R., and B. Kachar. 1990. Polarity and velocity of sliding filaments: control of direction by actin and of speed by myosin. *Science (Wash. DC).* 249:406–408.

Sellers, J. R., Y. J. Han, and B. Kachar. 1991. Movement of actin filaments by purified molluscan myosin and native thick filaments. *Biopys. J.* 59: 187a.

Sheetz, M. P., and J. A. Spudich. 1983. Movement of myosin-coated fluorescent beads on actin cables in vitro. *Nature (Lond.).* 303:31–35.

Shimmen, T., and M. Yano. 1984. Active sliding movement of latex beads coated with skeletal muscle myosin on *Chara* actin bundles. *Protoplasma.* 121:132–137.

Spudich, J. A., and S. Watt. 1971. The regulation of rabbit skeletal muscle contraction I. Biochemical studies of the interaction of the tropomyosin-troponin complex with actin and the proteolytic fragments of myosin. *J. Biol. Chem.* 246:4866–4871.

Sutoh, K., M. Ando, K. Sutoh, and Y. Y. Toyoshima. 1991. Site-directed mutations of *Dictyostelium* actin: disruption of a negative charge cluster at the N terminus. *Proc. Natl. Acad. Sci. USA.* 88:7711–7714.

Svoboda, K., C. F. Schmidt, D. Branton, and S. M. Block. 1992. Conformation and elasticity of the isolated red blood cell membrane skeleton. *Biophys. J.* 63:784–793.

Szent-Györgyi, A. G., C. Cohen, and D. E. Philpott. 1960. Light meromyosin fraction I: a helical molecule from myosin. *J. Mol. Biol.* 2: 133–142.

Toyoshima, Y. Y., S. J. Kron, E. M. McNally, K. R. Niebling, C. Toyoshima, and J. A. Spudich. 1987. Myosin subfragment-1 is sufficient to move actin filaments in vitro. *Nature (Lond.).* 328:536–539.

Toyoshima, Y. Y., S. J. Kron, and J. A. Spudich. 1990. The myosin step size: measurement of the unit displacement per ATP hydrolyzed in an in vitro assay. *Proc. Natl. Acad. Sci. USA.* 87:7130–7134.

Toyoshima, Y. Y., C. Toyoshima, and J. A. Spudich. 1989. Bidirectional movement of actin filaments along tracks of myosin heads. *Nature (Lond.).* 341:154–156.

Umemoto, S., A. R. Bengur, and J. R. Sellers. 1989. Effect of multiple phosphorylations of smooth muscle and cytoplasmic myosins on movement in an in vitro motility assay. *J. Biol. Chem.* 264:1431–1436.

Uyeda, T. Q. P., S. J. Kron, and J. A. Spudich. 1990. Myosin step size estimation from slow sliding movement of actin over low densities of heavy meromyosin. *J. Mol. Biol.* 214:699–710.

Uyeda, T. Q. P., H. M. Warrick, S. J. Kron, and J. A. Spudich. 1991. Quantized velocities at low myosin densities in an in vitro motility assay. *Nature (Lond.).* 352:307–311.

Vale, D. R., and F. Oosawa. 1990. Protein motors and maxwell's demons: does mechanochemical transduction involve a thermal ratchet?. *Adv. Biophys.* 26:97–134.

Wagner, P. D., and E. Giniger. 1981. Calcium-sensitive binding of heavy meromyosin to regulated actin in the presence of ATP. *J. Biol. Chem.* 256:12647–12650.

Warshaw, D. M., J. M. Desrosiers, S. S. Work, and K. M. Trybus. 1991. Effects of MgATP, MgADP, and Pi on actin movement by smooth muscle myosin. *J. Biol. Chem.* 266:24339–24343.

Yamada, T., O. Abe, T. Kobayashi, and H. Sugi. 1993. Myofilament sliding per ATP movement in rabbit muscle fibers studied using laser flash photolysis of caged ATP. *J. Physiol. (Lond.).* 466:229–243.

Yamada, A., N. Ishii, and K. Takahashi. 1990. Direction and speed of actin filaments moving along thick filaments isolated from molluscan smooth muscle. *J. Biochem.* 108:341–343.

Yamada, A., and K. Takahashi. 1992. Sudden increase in speed of an actin filament moving on myosin cross-bridges of "mismatched" polarity observed when its leading end begins to interact with cross-bridges of "matched" polarity. *J. Biochem.* 111:676–680.

Yamada, A., and T. Wakabayashi. 1993. Movement of actin away from the center of reconstituted rabbit myosin filament is slower than in the opposite direction. *Biopys. J.* 64:565–569.

Yanagida, T. 1993. Myosin orientation-dependent force and step size. *Proc. 32nd Congress of the International Union of Physiological Sciences.* Aug. 1–6. p.10.

Yanagida, T., T. Arata, and F. Oosawa. 1985. Sliding distance of actin filament induced by a myosin crossbridge during one ATP hydrolysis cycle. *Nature (Lond.).* 316:366–369.

Yanagida, A., Y. Harada, and A. Ishijima. 1993. Nano-manipulation of actomyosin molecular motors in vitro: a new working principle. *Trends Biochem. Sci.* 18:319–324.

Yanagida, T., A. Ishijima, K. Saito, and Y. Harada. Coupling between ATPase, and force- generating attachment-detachment cycles of actomyosin in vitro. *In* Mechanism of Myofilament Sliding in Muscle Contraction. H. Sugi, editor. Plenum/New York. 1993.

Yanagida, T., M. Nakase, K. Nishiyama, and F. Oosawa. 1984. Direct observation of motion of single F-actin filaments in the presence of myosin. *Nature (Lond.).* 307:58–60.

Yano, M. 1978. Observation of steady streamings in a solution of Mg-ATP and acto-heavy meromyosin from rabbit skeletal muscle. *J. Biochem.* 83:1203–1204.